

# Neuromorphic capacitive tactile sensors inspired by slowly adaptive mechanoreceptors

Ella Janotte<sup>1,2,\*</sup>, Simeon Bamford<sup>1</sup>, Ole Richter<sup>2,3</sup>, Maurizio Valle<sup>4</sup>, Chiara Bartolozzi<sup>1</sup>

**Abstract**—The sense of touch is essential in our everyday life as it allows us to interact with our environment. The same applies to robots and users of prostheses but requires sensing solutions that are power efficient and allow edge and embedded computation. In this paper, we present a capacitive, neuromorphic, event-driven, tactile sensor. The mixed-mode subthreshold circuit is implemented in 180 nm technology and achieves a sensitivity of  $\approx 30 \text{ Hz/N}$  in simulation with the SPICE simulation platform spectre.

**Index Terms**—Event-driven tactile sensor, Neuromorphic circuits, Asynchronous CMOS 180-nm technology, Leaky integrate and fire neuron, Capacitive

## I. INTRODUCTION

In humans, touch is one of the earliest developed senses [1]. It allows us to modulate contact forces when handling objects, identify textures and shapes, even blindfolded, and actively explore our environment. Mechanoreceptors of the human hairless skin are broadly divided into two categories, encoding either contact force (slowly adapting mechanoreceptor (SA)), or change in contact force (rapidly adapting mechanoreceptor (RA)) into spikes. Together, the activity of the different types of mechanoreceptors supports the perception of many different tactile features and qualities [2]. Tactile sensing is becoming increasingly important in the fields of robotics, prosthetics, IoT and many others. It allows robots to safely interact with their environment and improve performance in grasping and manipulation, and it allows prosthesis users to feel the objects they manipulate [3], [4]. Unlike in biology, artificial tactile sensors are conventionally sampled periodically, and a scalar pressure value is returned. However, a high enough sampling rate is needed to ensure no significant contact is missed or communicated with delay. However, in periods without contact, the sensors produce redundant data, the volume of which increases with the sampling rate.

In event-driven sensor arrays by contrast, and similarly to biological sensing, each sensor operates asynchronously and locally encodes change or stimulus intensity information into

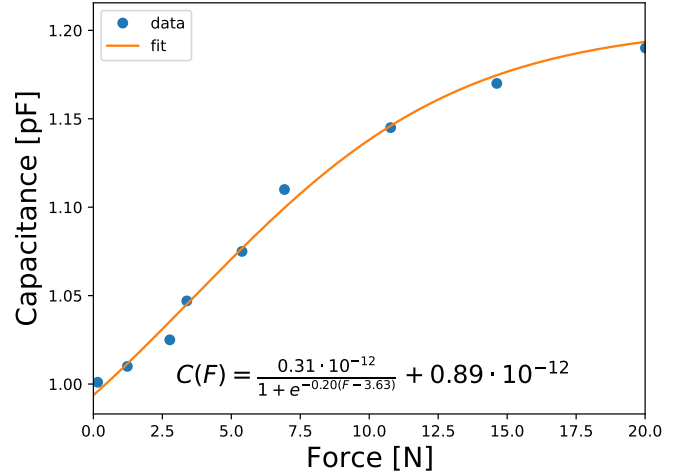


Fig. 1. The capacitance model is based on the iCub fingertip and fitted to measurements conducted with the omega.3 robot. The blue dots represent the experimental data points and the orange line is defined by the fitted function.

binary events [5]. The advantage of these sensors is their dynamic temporal resolution, which adapts to the stimulus by increasing the sampling rate when needed and decreasing the output activity for stationary inputs. They are characterised by energy efficiency, partly due to system-level energy saving through less data processing, and partly due to operation in the mixed-mode subthreshold regime whereby analogue computations are performed with very low currents. There are examples of these sensors in the visual, auditory, olfactory and tactile modalities [6]–[8].

There are several event-driven implementations of tactile sensors using resistive, capacitive and piezoelectric transducers. However, many of them are implemented using post-processing methods on FPGAs or uC for periodically sampled sensors. While these implementations can serve as tools for system-level application development [8]–[11], they do not reach the same low-power performance and miniaturisation as their mixed-mode subthreshold counterparts.

Currently, mixed-mode subthreshold tactile circuits implemented are based on piezoelectric transduction [12], [13], excluding opto-tactile neuromorphic sensors, which are an interesting alternative class of device, but having their own challenges (geometrical, illumination etc) [14]. While piezoelectric transducers are well suited for detecting fast changes and emulate the behaviour of rapidly adapting mechanoreceptors (RAs) in combination with change detection circuitry [13], their

This work has been funded by European Union's Horizon 2020 MSCA Programme under Grant Agreement No 813713 (Neutouch).

Affiliations: <sup>1</sup> Istituto Italiano di Tecnologia, Via San Quirico 19 D, Genova, Italy.

<sup>2</sup> Bio-Inspired Circuits and Systems (BICS) Group, Zernike Institute for Advanced Materials (ZIAM), Faculty of Science and Engineering (FSE), University of Groningen, Nijenborgh 4, NL-9747 AG Groningen, Netherlands.

<sup>3</sup> CogniGron (Groningen Cognitive Systems and Materials Center), University of Groningen, Nijenborgh 4, NL-9747 AG Groningen, Netherlands.

<sup>4</sup> Department of Electrical, Electronic and Telecommunication Engineering and Naval Architecture (DITEN), University of Genoa, Via Opera Pia 11, 16145 Genoa, Italy.

\* Corresponding author: ella.janotte@iit.it

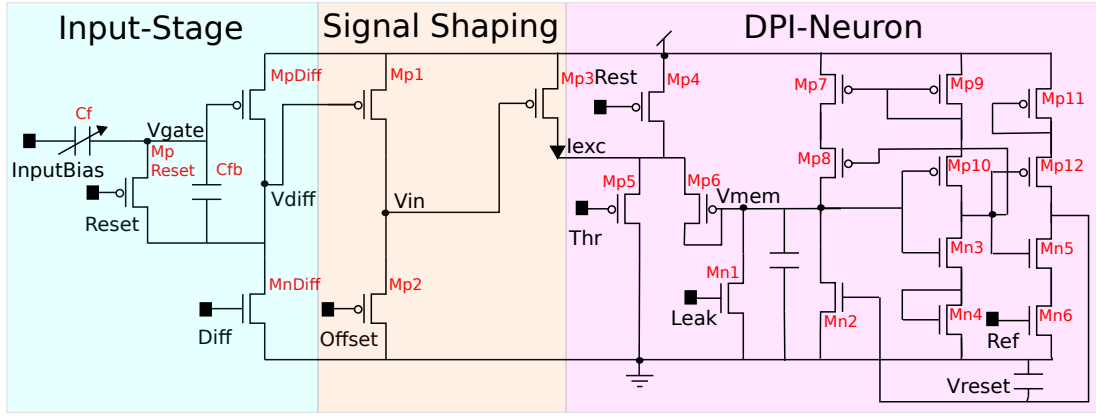


Fig. 2. The proposed readout circuit for a mixed-mode subthreshold capacitive event-driven force intensity sensor. The circuit is comprised of an input stage (blue), a signal shaping stage (orange) and a DPI-neuron (pink). Bias voltages provided to the circuit are marked by rectangles.

suitability for an intensity readout emulating the behaviour of slowly adapting mechanoreceptors (SAs) is limited to the time of change because the charge generated due to pressure dissipates over time. Capacitive transducers have, instead, the advantage of keeping their capacitance vs. time, and remaining passive components without constantly drawing current and dissipating energy (unlike resistive and inductive transducers).

Commonly, the readout of capacitive sensors is clocked [15], and the capacitance is inferred by the time necessary to charge and discharge the capacitor. In this study, we developed a mixed-mode subthreshold circuit that can continuously monitor the capacitance value and encode the absolute capacitance value into spike rates. This type of encoding loosely emulates the behaviour of SAs. The circuit has been designed in CADENCE with X-FAB XP018 technology, simulated with the SPICE simulation platform spectre and sent to production. In this paper, we describe the circuit, explain its working principle and present its characterisation by means of transient simulations. We show that the circuit responds to forces in a range between 0 N and 20 N, with a sensitivity of up to 28.62 Hz/N, at a power consumption of 777 nW.

In combination with the previously proposed piezoelectric neuromorphic tactile sensors loosely reproducing the behaviour of RA, the capacitive neuromorphic sensors loosely inspired on the SA can enrich the encoding capability of artificial tactile sensing within a single low-power device. This is especially important in tactile feedback in prosthetic devices, where the elicited sensation is more natural for stimulation reproducing the characteristic firing pattern of RA and SA [16].

TABLE I  
DIMENSIONS OF THE USED TRANSISTORS.

Transistor	Width	Length
$Mp_{Diff}, Mn_{Diff}$	2.2u	4.4u
$Mp_1, Mp_2$	2u	4u
$Mp_{reset}$	250n	2u
Neuron	2u	2u

## II. METHODS

The neuromorphic capacitive sensor is shown in Fig. 2. It is composed of an input and amplification stage, a signal shaping stage and a spike generation stage (the DPI-neuron [17], [18]). The capacitor changes capacitance due to the application of force and subsequent deformation. The input stage, [19], translates the value of capacitance into a voltage. The dimensions of the transistors are presented in Table I and optimized for the correct capacitance scaling and mismatch.

The coupling between the sensing capacitor  $C_f$  and  $C_{fb}$  amplifies the capacitance value with respect to its idle state value. The  $Mp_{Reset}$  transistor resets the circuit at the beginning of operation to set the resting potential of  $V_{diff}$  and  $V_{gate}$ . When the capacitance changes, charge moves onto  $V_{gate}$ . The amplified change is reflected in  $V_{diff}$  which serves as input to the signal shaping stage. In this stage, the voltage that correlates with the input force is converted into a current fed to the output DPI-neuron that converts it into a spike train with an instantaneous firing rate proportional to the input force.

To initialise the circuit before use,  $Mp_{Reset}$  is turned on, and the nodes  $V_{gate}$  and  $V_{diff}$  are shorted, defining  $V_{gate}$  as the voltage which allows  $Mp_{Diff}$  to source as much current as  $Mn_{Diff}$  sinks. Once the reset transistor is turned off, any change in the sensing capacitance  $C_f$  will result in a movement of charge onto  $V_{gate}$ . The voltage difference between the  $InputBias$  and the resting voltage of  $V_{gate}$  introduces an amplification of the change in capacity on  $V_{gate}$ . In our implementation, the change in that node is then compensated by feedback across  $C_{fb}$ , resulting in a further amplification with the ratio of  $C_f / (C_{fb} + C_{MpDiff})$  onto the node  $V_{diff}$ . The advantage of including  $C_{fb}$  is that the amplification ratio of the circuit is well matched to the sensing  $C_f$ .

In a simplified model, without the signal shaping stage,  $V_{diff}$  would directly drive  $Mp_3$  to produce  $I_{exc}$  and charge the neuron. However, depending on the sign of  $InputBias - V_{gate}(t_0)$ ,  $V_{diff}$  will increase with force (negative) or decrease with force (positive). While the high  $InputBias$  would enable a readout where the frequency increases with input force (for a standard LIF implementation), it would also introduce the neuron to

high  $I_{exc}$  in the resting state. Hence, a stage that removes that offset is advisable. Since for most  $V_{diff}$  configurations, the resting  $V_{diff}$  ranges between roughly 1.2 V and 1.4 V we chose to operate with an *InputBias* smaller than that, to allow for a wider range of operation.

Hence, in the presented circuit with an increase in force,  $V_{diff}$  will increase. However, if the circuit shall exhibit increasing spike rates over increasing pressure, then the voltage driving the input transistor to the LIF must decrease with increasing force for our standard LIF implementation. The second stage of the circuit facilitates this conversion. Unlike in a p-type source-follower, the  $Mp_1$  does not function as the fixed current source but as the input transistor. The gate of  $Mp_2$  instead is provided with a constant voltage. Following Kirchhoff's law, the current through both transistors must be the same. Assuming that both transistors stay in saturation, for  $Mp_2$ , to permit the current,  $|V_{in} - Offset| = |V_{dd} - V_{diff}|$ . Thus,  $V_{in}$  must decrease, when  $V_{diff}$  increases. Depending on the biasing of this circuit, the offset and slope of the current fed to the neuron and, hence, the output firing rate of the neuron can be modulated, trading off sensitivity, saturation and mean activity of the neuron.

Finally,  $V_{In}$  modulates the input current to the DPI-leaky integrate-and-fire neuron (LIF) neuron ( $I_{exc}$ ) that translates the current into a spike train. In the integration process of the DPI neuron, the diode connection of  $Mp_6$  leads to a saturating process that decreases the effect of the input current for  $V_{mem}$  close to the firing threshold of the neuron.

The circuit was characterized with transient simulations with spectre, using transistor models from X-FAB XP018 design kit. The model of the capacitive transducer is based on the iCub robot's fingertip. The sensors are a sandwich consisting of electrodes printed on a flexible PCB and a three-layer fabric combining a dielectric layer, a conductive layer connected to ground, and a protective top layer [20]. The model of capacitance vs force, shown in Fig. 1, is fitted from measurement data collected with an Omega.3 robot [21], neglecting the fabric's time response due to the setup's limited time response. The obtained force-capacitance equation was implemented in VERILOG-A and integrated into the circuit simulation.

### III. RESULTS

Fig. 3 shows the circuit's transient response to constant input forces, ranging from 0 N to 10 N in step increments and decrements of 2 N. We measured the voltages  $V_{gate}$ ,  $V_{diff}$ ,  $V_{in}$  and the neuron's instantaneous firing rate. At time  $t = 1$  s (marked by the red bar) the reset pulse connects  $V_{gate}$  and  $V_{diff}$ , that reach the same resting-state voltage. Once the force is applied,  $V_{diff}$  changes more strongly than  $V_{gate}$  due to the amplification introduced by the coupled capacitors. Once the force is removed, they move to share the same resting-state voltage again. When the force increases,  $V_{diff}$  increases and  $V_{in}$  decreases; vice-versa, when  $V_{diff}$  drops after the withdrawal of the force,  $V_{in}$  rises back to its resting voltage. The neuron's spiking activity increases with increasing force and goes back

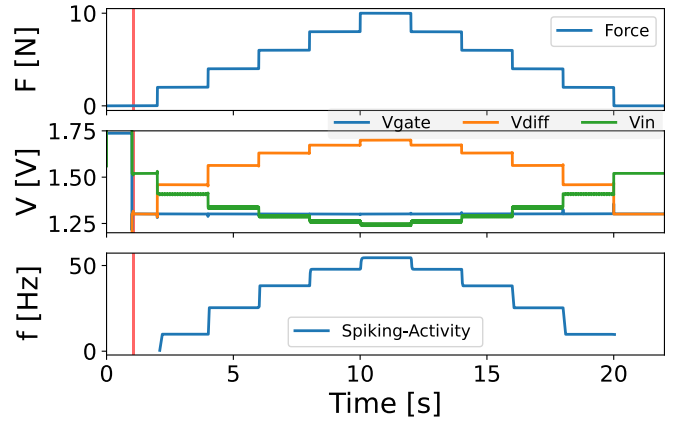


Fig. 3. Neuromorphic capacitive sensor transient behaviour: The red bar at 1 s indicates the timing of the reset pulse. Top: Force input to the circuit in increments of 2 N every two seconds. Middle:  $V_{gate}$  (blue),  $V_{diff}$  (orange) and  $V_{in}$  (green). Bottom: Instantaneous mean firing rate, computed as the inverse of the inter-spike interval. It can only be computed when two spikes occur, i.e. when a force is applied and the change of the capacitance is large enough.

to zero after the force's withdrawal, matching the input force's behaviour. While the force vs frequency behaviour shows non-linearity (saturation of frequency), it follows the behaviour of the capacitive transducer shown in Fig. 1.

We characterized the impact of the *Offset* voltage on the circuit's spiking behaviour and power consumption vs the input force. Fig. 4 shows the circuit's spike rate (inverse of the inter-spike interval, in red) and the power consumption (in blue) in response to step-forces from 0 N to 20 N in increments of 0.5 N, for *Offset* corresponding to 0.6 V, 0.8 V and 1.0 V. The instantaneous firing rate roughly follows the shape of the capacitance vs. force, increasing with increasing force and saturating for high forces. However, the three curves differ strongly in the sensitivity they provide and the spike rate for no force input. For *Offset* = 1.0 V, the circuit starts to slowly spike at forces around 2 N and saturates at 10 N. In contrast, for *Offset* = 0.8 V, the circuit is already sensitive to low forces and allows their differentiation but also rapidly saturates at 10 N where higher forces can no longer be distinguished. Further decreasing the offset to *Offset* = 0.6 V increases the circuit's dynamic range, as the frequency response covers at least three times the range obtained with lower offsets. While the curve transitions towards saturation at 10 N as well, the transition is more gradual and still allows for differentiation at high forces. However, when no force is applied, the circuit still spikes at roughly 30 Hz. While this offset could be removed by increasing the neuron's leaking current, that increase would further increase the static power consumption. The blue curves show clearly that the power consumption increases with increasing force and decreasing *Offset*, respectively. The circuit's sensitivity, idle spiking frequency and power consumption for the different *Offset* voltages are reported Table II.

Fig. 5 qualitatively compares the circuit's output to the behaviour of SA as reported by [22]. The circuit receives a similarly shaped input as the biological mechanoreceptors. The

TABLE II  
COMPARISON OF *Offset* PROPERTIES.

<i>Offset</i>	0.6 V	0.8 V	1.0 V
Sensitivity	28.6 Hz/N	9.17 Hz/N	3.94 Hz/N
Idle Frequency	35.6 Hz	1.46 Hz	0 Hz
Power	777 nW	83.5 nW	6.20 nW

instantaneous firing rate of the circuit matches the force input for the whole stimulus duration. In contrast, the Merkel cell (SAI) fires most rapidly in the up-ramping of the stimulus, and the cell's activity decreases with time during constant stimulation. The circuit's behaviour is closer to that of the Ruffini corpuscle (SAII), which increases activity with increasing stimulus intensity and keeps a consistent firing rate for constant stimulation. The corpuscle stops spiking at the onset of the downward ramp. While the behaviour is not matched perfectly, the circuit behaves remarkably similar to the SAII.

#### IV. CONCLUSIONS

This paper showed the basic functionality of a neuromorphic, event-driven, capacitive tactile sensor that is not limited to a fixed sampling rate. The circuit enables a capacitive intensity readout with tunable sensitivity. An increase in sensitivity is traded off with higher power consumption. However, the circuit flexibility allows system designers to define their requirements, adapting the circuit behaviour to the application at hand. The high resting frequency for *Offset* = 0.6 V could be reduced by increasing the neuron's leak current. While this would increase the power consumption in the resting state, the decrease in spikes would decrease the necessary computational power and transmission bandwidth at a system level.

The presented preliminary results show the circuit's main functionality in converting the input force into an informative spike train that closely resembles the behaviour of biological tactile sensors. When available, a deeper characterization and exploration of the parameter space will be performed with a circuit prototype. Specifically, we will explore biases of the

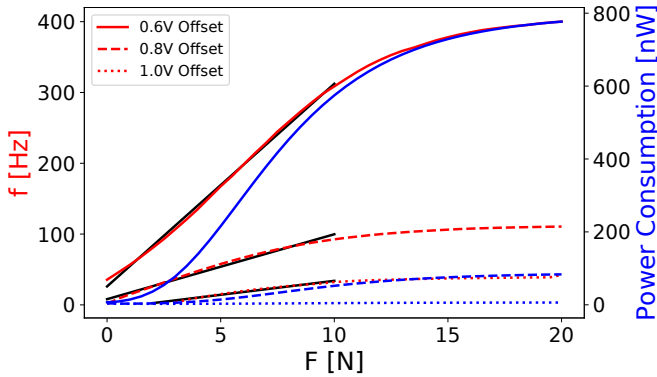


Fig. 4. Capacitive neuromorphic sensor output frequency (red) and power consumption (blue) vs input force for varying *Offset* voltages. The black lines indicate the sensor's resolution for each bias setting and their y-intercepts indicate the resting state frequencies. The sensor's sensitivity, spike rate and power consumption increases with decreasing *Offset*.

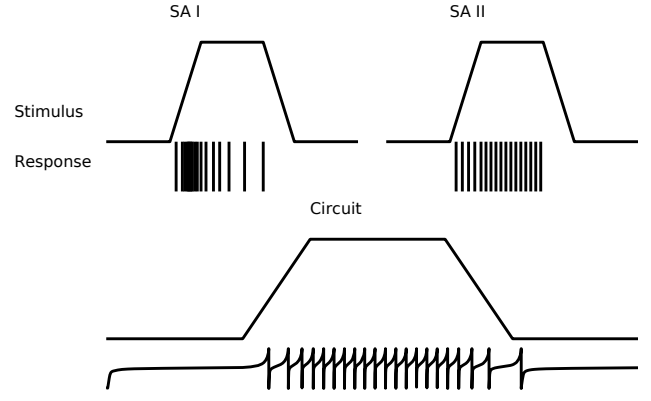


Fig. 5. Qualitative comparison with biological tactile afferents: (top) Response of the two types of SA found in hairless human skin, Merkel cells (SAI, on the left) and Ruffini corpuscles (SAII, on the right), to stimulation. (bottom) Membrane potential of the DPI-neuron in the neuromorphic capacitive sensor in response to stimulation. The peaks correspond to the action potentials shown as vertical bars in the top plots.

neuron that could further change the shape of the signal, such as the DPI gain (*Thr*), the offset of the resting firing rate (*Leak*) and the refractory period (*Ref*).

The circuit could further be extended to achieve a higher level of biological plausibility. One possible extension could provide self-inhibitory feedback, enabling the spike-rate adaptation for continuous inputs characteristic of SAI mechanoreceptors. To emulate the behaviour of the change-sensitive rapidly adapting mechanoreceptors (RAs) it could further be possible to connect the neuron's reset to the input-stage reset. That connection would reset  $V_{gate}$  after every spike and thus encode change in force. Although this neuron directly resets itself, it would be possible to perform reset via an asynchronous digital communication protocol, guaranteeing the delivery of spikes to downstream circuitry.

Once we receive the produced circuit on-chip, we will further evaluate the possibility and impact of leak in  $Mp_{Reset}$  and the resulting drift in  $V_{gate}$ . For the experiments with the circuit on chip, the biases will be generated by a parameter generator on chip inspired by [6]. Depending on the strength of the leak, one way to deal with it could be to apply regular reset pulses, or if the leak is too fast, the circuit could be transformed into a change-detecting circuit.

We have shown that with the proposed circuit, we can read out force intensities with a capacitive transducer without being limited by a frame rate, with a measured sensitivity of up to 28.6 Hz/N.

#### V. ACKNOWLEDGEMENT

The authors would like to acknowledge and thank Elisabetta Chicca and Michele Mastella for the fruitful discussions and support.

#### REFERENCES

- [1] G. Gottlieb, "Ontogenesis of sensory function in birds and mammals," *The biopsychology of development*, pp. 67–128, 1971.
- [2] H. P. Saal and S. J. Bensmaia, "Touch is a team effort: interplay of submodalities in cutaneous sensibility," *Trends in Neurosciences*, vol. 37, no. 12, pp. 689–697, 2014.

- [3] C. M. Oddo, L. Beccai, J. Wessberg, H. B. Wasling, F. Mattioli, and M. C. Carrozza, "Roughness Encoding in Human and Biomimetic Artificial Touch: Spatiotemporal Frequency Modulation and Structural Anisotropy of Fingerprints," *Sensors*, vol. 11, no. 6, pp. 5596–5615, 2011.
- [4] E. D'anna, F. M. Petrini, F. Artoni, I. Popovic, I. Simanić, S. Raspopovic, and S. Micera, "A somatotopic bidirectional hand prosthesis with transcutaneous electrical nerve stimulation based sensory feedback," *Scientific reports*, vol. 7, no. 1, pp. 1–15, 2017.
- [5] S.-C. Liu and T. Delbruck, "Neuromorphic sensory systems," *Current opinion in neurobiology*, vol. 20, no. 3, pp. 288–295, 2010.
- [6] S.-C. Liu, T. Delbruck, G. Indiveri, A. Whatley, and R. Douglas, *Event-based neuromorphic systems*. John Wiley & Sons, 2014.
- [7] A. Vanarse, A. Osseiran, and A. Rassau, "A review of current neuromorphic approaches for vision, auditory, and olfactory sensors," *Frontiers in neuroscience*, vol. 10, p. 115, 2016.
- [8] W. W. Lee, S. L. Kukreja, and N. V. Thakor, "A kilohertz kilotaxel tactile sensor array for investigating spatiotemporal features in neuromorphic touch," in *2015 IEEE Biomedical Circuits and Systems Conference (BioCAS)*. IEEE, 2015, pp. 1–4.
- [9] W. W. Lee, Y. J. Tan, H. Yao, S. Li, H. H. See, M. Hon, K. A. Ng, B. Xiong, J. S. Ho, and B. C. Tee, "A neuro-inspired artificial peripheral nervous system for scalable electronic skins," *Science Robotics*, vol. 4, no. 32, p. eaax2198, 2019.
- [10] S. Prasanna, L. Massari, E. Sinibaldi, R. Detry, J. Bowkett, K. Carpenter, and C. M. Oddo, "Neuromorphic tactile sensor array based on fiber bragg gratings to encode object qualities," in *Optics and Photonics for Information Processing XIII*, vol. 11136. International Society for Optics and Photonics, 2019, p. 1113608.
- [11] C. Bartolozzi, P. M. Ros, F. Diotalevi, N. Jamali, L. Natale, M. Crepaldi, and D. Demarchi, "Event-driven encoding of off-the-shelf tactile sensors for compression and latency optimisation for robotic skin," in *2017 IEEE/RSJ International Conference on Intelligent Robots and Systems (IROS)*. IEEE, 2017, pp. 166–173.
- [12] S. Caviglia, L. Pinna, M. Valle, and C. Bartolozzi, "An event-driven posfet taxel for sustained and transient sensing," in *2016 IEEE International Symposium on Circuits and Systems (ISCAS)*. IEEE, 2016, pp. 349–352.
- [13] A. Abou Khalil, M. Valle, H. Chible, and C. Bartolozzi, "Cmos dynamic tactile sensor," in *2017 New Generation of CAS (NGCAS)*. IEEE, 2017, pp. 269–272.
- [14] B. Ward-Cherrier, N. Pestell, and N. F. Lepora, "Neurotac: A neuromorphic optical tactile sensor applied to texture recognition," in *2020 IEEE International Conference on Robotics and Automation (ICRA)*. IEEE, 2020, pp. 2654–2660.
- [15] Y. Yoo and B.-D. Choi, "Readout circuits for capacitive sensors," *Micromachines*, vol. 12, no. 8, p. 960, 2021.
- [16] G. Valle, A. Mazzoni, F. Iberite, E. D'Anna, I. Strauss, G. Granata, M. Controzzi, F. Clemente, G. Rognini, C. Cipriani *et al.*, "Biomimetic intraneural sensory feedback enhances sensation naturalness, tactile sensitivity, and manual dexterity in a bidirectional prosthesis," *Neuron*, vol. 100, no. 1, pp. 37–45, 2018.
- [17] C. Bartolozzi and G. Indiveri, "Synaptic dynamics in analog vlsi," *Neural computation*, vol. 19, no. 10, pp. 2581–2603, 2007.
- [18] P. Livi and G. Indiveri, "A current-mode conductance-based silicon neuron for address-event neuromorphic systems," in *2009 IEEE international symposium on circuits and systems*. IEEE, 2009, pp. 2898–2901.
- [19] P. Lichtsteiner, C. Posch, and T. Delbruck, "A  $128 \times 128$  120 db 15  $\mu$ s latency asynchronous temporal contrast vision sensor," *IEEE journal of solid-state circuits*, vol. 43, no. 2, pp. 566–576, 2008.
- [20] N. Jamali, M. Maggiali, F. Giovannini, G. Metta, and L. Natale, "A new design of a fingertip for the icub hand," in *2015 IEEE/RSJ International Conference on Intelligent Robots and Systems (IROS)*. IEEE, 2015, pp. 2705–2710.
- [21] F. Dimension. (2022) Omega.3 robot. [Online]. Available: <https://www.forcedimension.com/products/omega>
- [22] L. J. Drew, F. Rugiero, and J. N. Wood, "Touch," in *Current topics in membranes*. Elsevier, 2007, vol. 59, pp. 425–465.